# Metastable MnS Crystallites through Solvothermal Synthesis

Jun Lu,† Pengfei Qi,† Yiya Peng,† Zhaoyu Meng,† Zhiping Yang,† Weichao Yu,† and Yitai Qian*,†,‡

*Structure Research Laboratory and Department of Chemistry, University of Science and Technology of China, Hefei, Anhui 230026, P.R. China*

*Received January 19, 2001. Revised Manuscript Received March 26, 2001*

Metastable ($\beta$ and $\gamma$) and stable ($\alpha$) MnS crystallites were synthesized by solvothermal reaction in various solvents at 190−200 °C. In tetrahydrofuran and benzene, the metastable MnS crystallites can be obtained. In water, ammonia liquor, ethylenediamine, $\alpha$-MnS, which is converted from the metastable phase, would be obtained. The low solubility of MnS is the crucial reason to stabilize the metastable phase with good yield. The metastable MnS crystallites were characterized by X-ray diffraction, X-ray photoelectron spectroscopy, and transmission electron microscopy. The metastable $\gamma$-MnS crystallites with rodlike morphology were found, and a unique "methane-like" four-branched rod cluster was characterized. The blue shift of the absorption edge indicates the quantum size effect of metastable MnS nanocrystallites.

## 1. Introduction

Group II−VI semiconductor nanomaterials have been the subject of intense researches for the past 10 years. Group II−VI semiconductors with Mn doping such as (Zn, Mn) and (Cd, Mn) chalcogenide mixed crystals are typical and the most extensively studied diluted magnetic semiconductors (DMS), which show unique magnetooptical properties caused by a strong s,p−d exchange interaction between electron/hole band states and $Mn^{2+}$ 3d electron states.[1,2] In these materials there is also an antiferromagnetic correlation between the $Mn^{2+}$ ($S = {}^5/_2$) spins due to d−p−d superexchange interaction.[3,4] In recent years, for both basic and applicative reasons, especially in blue/green light emitters,[5] DMS found continuously growing interest[6−10] which has been further stimulated by the successful preparation of multi-quantum-well structures and superlattices on the basis of these materials. This also stimulates researches concerning the pure Mn chalcogenides. Because of the zinc blend (ZB) and wurtzite (W) type structures of the mixed crystals, especially the optical properties of the tetrahedrally coordinated crystallographic modifications, the Mn chalcogenides (for MnS, metastable form) as limiting components are important.

Usually, MnS has three phases: $\alpha$-MnS is the green stable form (alabandite) with rock salt (RS) structure and $\beta$- and $\gamma$-MnS are pink metastable modifications with sphalerite and wurtzite (ZB/W) structures, respectively. Both of them are antiferromagnetic with the Néel temperature 152 K (RS) and 90 K (ZB/W), respectively. The poorly crystallized metastable form can be easily precipitated from an aqueous solution. Metastable MnS polycrystallites have been prepared in a thin film with a low substrate temperature ($T_s$ = 50 °C), above 100 °C,[11−13] or at high pressure,[14] they convert to the stable form. The direct growth of metastable MnS(W) and MnS(ZB) thin films has also been reported by gas source molecular−beam epitaxy (MBE; $T_s$ = 150−250 °C) onto GaAs(111)-[15] and -(100)[16]-oriented substrates, respectively. However, in most MBE technology, the gas source is toxic and the procedure is complicated. Recently, ZnY[17−19] and CdY[20−22](Y = S, Se, and Te) nanocrystallites with various morphologies (e.g., nanorods and nanowires) were prepared by solvothermal reactions.

* To whom correspondence should be addressed. E-mail: tslu@mail.ustc.edu.cn.
† Department of Chemistry.
‡ Structure Research Laboratory.

(1) Furdyna, J. K. *J. Appl. Phys.* **1988**, *64*, R29.
(2) Goede, O.; Heimbrodt, W. *Phys. Status Solidi B* **1988**, *146*, 11.
(3) Hass, K. C.; Ehrenreich, H. *J. Cryst. Growth* **1988**, *86*, 8.
(4) Larson, B. E.; Hass, K. C.; Ehrenreich, H.; Carlsson, A. E. *Solid State Commun.* **1985**, *56*, 347.
(5) Gunshor, R. L.; Nurmikko, A. V. *Semiconductors and Semimetals*; Academic: New York, 1997; Vol. 44.
(6) Gaj, J. A. *J. Phys. Soc. Jpn., Suppl.* A **1980**, *49*, 747.
(7) Furdyna, J. K. *J. Appl. Phys.* **1982**, *53*, 7637.
(8) Brandt, N. B.; Moshchalkov, V. V. *Adv. Phys.* **1984**, *33*, 193.
(9) Galazka, R. R. *J. Cryst. Growth* **1985**, *72*, 364.
(10) Furdyna, J. K. *J. Vacuum Sci. Technol. A* **1986,** *4*, 2002.
(11) Goede, O.; Heimbrodt, W.; et al. *Phys. Status Solidi B* **1987**, *143*, 511.
(12) Rooymans, C. J. M. *Adv. High Pressure Res.* **1969**, *2*, 1.
(13) Futuseth, S.; Kjekshus, A. *Acta Chem. Scand.* **1965**, *19*, 1405.
(14) Kennedy, S. W.; Harris, K.; Summerville, E. *J. Solid State Chem.* **1980**, *31*, 355.
(15) Okajima, M.; Tohda, T. *J. Cryst. Growth* **1992**, *117*, 810.
(16) Skromme, B. J.; Zhang, Y.; Smith, D. J.; Sivananthan, S. *Appl. Phys. Lett.* **1995**, *67*, 2690.
(17) Li, Y.; Ding, Y.; Zhang, Y.; Qian, Y. *J. Phys. Chem. Solids* **1999**, *60*, 13.
(18) Li, Y. D.; Ding, Y.; Qian, Y. T.; Yang, L.; Zhang, Y. *Inorg. Chem.* **1998**, *37*, 2844.
(19) Li, Y. D.; Ding, Y.; Wang, Z. Y. *Adv. Mater.* **1999**, *11*, 847.
(20) Yu, S. H.; Wu, Y. S.; Yang, J.; Qian, Y. T.; et al. *Chem. Mater.* **1998**, *10*, 2309.
(21) Yu, S. H.; Yang, J.; Han, Z. H.; Qian, Y. T.; et al. *J. Mater. Chem.* **1999**, *9*, 1283.
(22) Yan, P.; Xie, Y.; Qian, Y. T.; Liu, X. M. *Chem. Commun.* **1999**, 1293.

10.1021/cm010049j CCC: $20.00 
Published on Web 06/01/2001

**Table 1. Product Phase of Solvothermal Reaction (1)**

| | time (h) | | | | |
|---|---|---|---|---|---|
| solvent | 2 | 4 | 6 | 9 | 12 |
| benzene | W | | | | W |
| THF | *a* | *a* | ZB | ZB | ZB |
| $H_2O$ | *a* | W + RS | W + RS | | RS |
| $NH_3 \cdot H_2O$ | W + RS | | | | RS |
| en | W + RS | RS | | | RS |

[a] No product is obtained.

In this paper to be described, with thiourea as the sulfur resource, the MnS crystallites were prepared by solvothermal reaction at 190−200 °C, which is slightly higher than the decomposition temperature of thiourea (180 °C). Three forms can be prepared with water (or ethylenediamine and ammonia liquor), benzene, and tetrahydrofuran (THF) as the solvent, respectively.

## 2. Experimental Section

**2.1. Chemicals.** $MnCl_2 \cdot 4H_2O$, 99.0%; $SC(NH_2)_2$, 99.0+%; benzene, 99.5%; THF, 99+%; ethylenediamine, 99.0%; absolute ethanol, 97.0+%; ammonia liquor, 25−28% for $NH_3$. All of the chemicals are analytical grade (from Shanghai Chemical Reagent Co., Ltd.) and were used as received without further purification.

**2.2. Syntheses.** The nanocrystalline MnS samples were prepared by the solvothermal method. Analytical-grade $MnCl_2 \cdot 4H_2O$ (1.99 g) and thiourea (3.04 g) with a 1:4 molar ratio were added into a Teflon-lined autoclave of 60 mL capacity, filling the autoclave with 50 mL of solvent. The autoclave was sealed into a stainless steel tank, maintained at 190−200 °C for 2−12 h, and then cooled to room temperature in air. The samples of MnS were filtered and washed with a solvent, distilled water, and absolute ethanol, respectively, to remove impurities and dried in a vacuum at 50 °C for 1 h. The yields based on $MnCl_2 \cdot 4H_2O$ are about 45% and 75% for metastable (ZB/W) and stable (RS) forms, respectively. The product phases are listed in Table 1.

**2.3. Instruments and Characterization.** *Powder X-ray Diffraction* (*XRD*). Powder XRD patterns were measured with a scanning rate of 8.0000°/min in the $2\theta$ range from 10° to 70°, using a MAX 18 AHF X-ray diffractometer (MAC Science Co., Ltd.) equipped with graphite-monochromatized Cu $K\alpha_1$ radiation ($\lambda$ = 1.540 56 Å). The lattice constants were fitted through the program of Cell Version 5.0 (Copyright by K. Dwight, USA, 1986).

*X-ray Photoelectron Spectroscopy* (*XPS*). XPS were recorded on a VGESCALAB MKII X-ray photoelectron spectrometer, using nonmonochromatized Mg Kα (1253.6 eV) X-ray in high vacuum ($5 \times 10^{-9}$ Pa), as the excitation source. The values of the binding energy ($E_B$) were calibrated with the C 1s peak (284.6 eV) as the internal standard.

*Transmission Electron Microscopy* (*TEM*). Samples for TEM were prepared by putting a few drops of an absolute ethanol solution of ultrasonically dispersed crystallite samples onto an amorphous carbon substrate supported on a copper grid and then allowing the solvent to evaporate at room temperature. TEM images and selected area electron diffraction (SAED) on samples and the energy-dispersive analysis of X-ray fluorescence (EDAX) were taken with an Hitachi model H-800 TEM, using an accelerating voltage of 200 kV.

*Optical Absorption Measurement*. The metastable MnS crystallites were ultrasonically dispersed in absolute ethanol, and the solutions were placed into silica cuvettes (1 cm). The optical absorption spectra were measured on a Specord 200 PC UV−vis spectrophotometer (Analytic Jena GmbH) with absolute ethanol as the reference.

## 3. Results and Discussion

The powder XRD patterns of MnS are shown in Figure 1. The samples in Figure 1a,b were prepared in benzene and THF, respectively. The diffraction peaks in Figure 1a,b can be indexed as the hexagonal MnS(W) with lattice constant $a$ = 3.9738 Å and $c$ = 6.4275 Å (Joint Committee on Powder Diffraction Standards (JCPDS), Powder Diffraction File No. 40-1289, $a$ = 3.9792 Å and $c$ = 6.4469 Å) and as the cubic MnS(ZB) with $a$ = 5.6121 Å (JCPDS, Powder Diffraction File No. 40-1288, $a$ = 5.6147 Å). The weak diffraction peak at $2\theta$ = 26.10° in Figure 1b is the 100 diffraction of the minor amount MnS(W) form. In Figure 1c, the XRD of the stable form MnS, which was hydrothermally synthesized, can be indexed as the cubic MnS(RS) with $a$ = 5.2242 Å (JCPDS, Powder Diffraction File No. 6-518, $a$ = 5.224 Å). The broadening of the diffraction peak indicates that the samples are nanoscale in size.

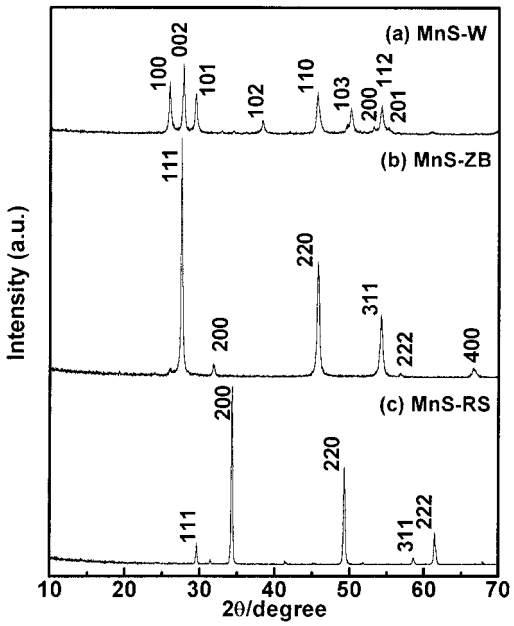


**Figure 1.** Powder XRD patterns of as-prepared MnS samples. The metastable form with W (a) and ZB (b) types and the stable form with RS type (c) were synthesized in benzene, THF, and water, respectively.

Parts a−c of Figure 2 are the Mn 2p region of the XPS of as-prepared MnS samples. The binding energy of Mn $2p_{3/2}$ with 640.85−641.05 eV in the metastable form (ZB/W) and with 641.35 eV in the stable form (RS) are, under the experimental error range, consistent with the reference values: 640.8 and 641.7 eV, respectively.[23] The S $2p_{3/2}$ peak at 161.20 eV in Figure 2d is also consistent with the reference value of MnS.[23] This value is distinctly lower than that found for other transition-metal monosulfides, indicating that MnS is more ionic in character (less delocalization of electrons into Mn 3d orbitals) than the first-row early-transition-metal monosulfides.[24] The XPS surface analysis also shows that the sulfur ions are ready to be oxidized; in fact, all of the samples are surface-absorbed with carbon and oxygen elements due to exposure to air during the processing of samples.

Figure 3 shows the TEM images and SAED pattern of the metastable MnS(W) sample. Figure 3a shows

(23) Muilenberg, G. E.; Wagner, C. D.; Riggs, W. M.; Davis, L. E.; Moulder, J. F. *Handbook of X-ray Photoelectron Spectroscopy*; Physical Electronics Division, Perkin-Elmer Corp.: New York, 1979; p 74.

(24) Franzen, H. F.; Umana, M. X. *J. Solid State Chem.* **1976**, *18*, 363.

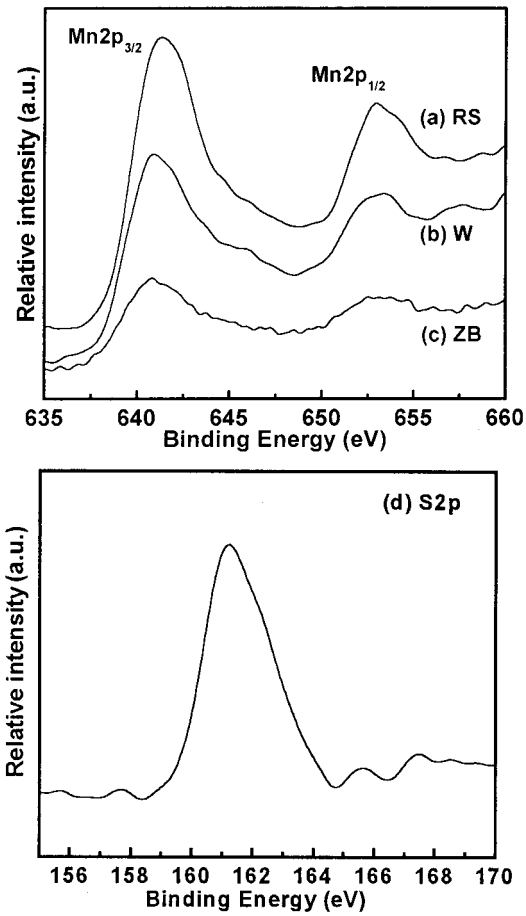


**Figure 2.** XPS of MnS crystallites: (a−c) Mn 2p region for stable (RS) and metastable (W/ZB) MnS crystallites, respectively; (d) S2p region for both of them.

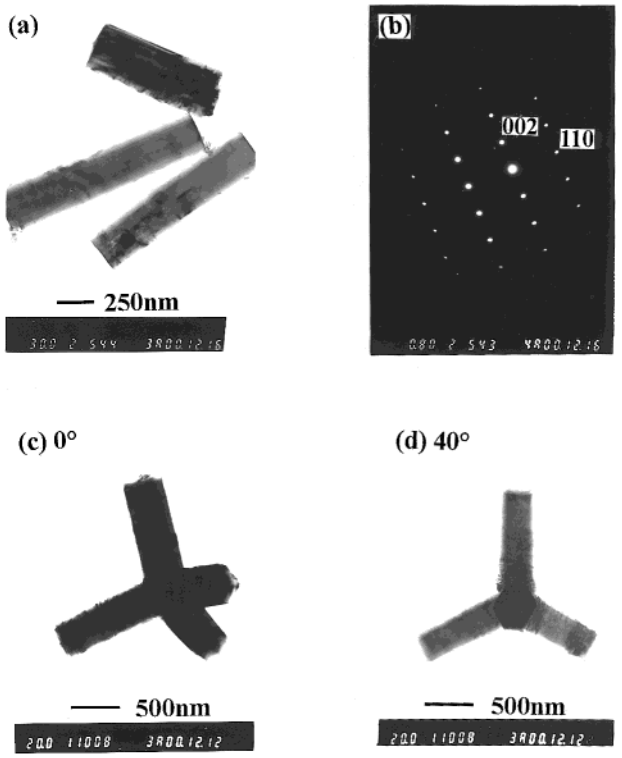


**Figure 3.** TEM images (a) and the SAED pattern (b) of rodlike MnS(W) crystallites. (c and d) TEM images of "methane-like" four-branched rod clusters of metastable MnS(W), which are taken when the sample plane is horizontal (0°) and tilted by 40°, respectively.

rodlike morphology with 20−300 nm of diameter and 1−2.5 $\mu$m of length; the SAED pattern of a rod in Figure 3b can be identified as the [$\bar{1}$10] zone axis projection of the MnS(W) reciprocal lattice. The atomic ratio Mn/S is estimated to be 0.74 through EDAX. Furthermore, we found an interesting morphology of MnS(W) crystallites as shown in Figure 3c, which can be called "methane-like" four-branched rod clusters. When the sample plane is tilted by 40°, we got a three-branched image (Figure 3d), with the angles between each axis of rod being 118°, 118° and 124°, respectively, approximately identical with 120°, which is the case when the electron beam is parallel with one of the branches. In Figure 3d, a hexagon is overlapping at the point of intersection of the rod cluster; because no hexagonal platelike crystallites are found in Figure 3c, the hexagon should be the image from the end section of one branch. From the SAED result in Figure 3b, it can be concluded that the rods grow along the *c* direction of the MnS(W) lattice. This orientation of the rods is the same as that found in CdSe crystallites with hexagonal wurtzite structure.[25] In the solvothermal condition with temperature higher than the decomposition temperature of thiourea (180 °C), the growth of metastable MnS(W) rods was kinetically driven by a high $H_2S$ concentration (Mn:S = 1:4) and a low solubility of metastable MnS. Furthermore, the anisotropy of MnS(W) crystallites with a unique *c* axis (closest stacking direction of ions) results in faster growth along the *c* axis than along other directions.[25] The growth mechanism of "methane-like" four-branched rod clusters is not very clear. However, cubic ZnS (ZB structure, point symmetry with $T_d$) has a growth habit of tetrahedral morphology enclosed by {111} crystallographic facets, because metastable MnS have the same phase relation as that of ZnS and two-phase coexistence (ZB/W) is familiar. We think that if the MnS(ZB) crystallizes as a tetrahedral crystal seed and the MnS(W) hexagonal phase grows on the surface of the seed, a "methane-like" rod cluster can result. More convictive evidences are needed, and further work is in progress. For the samples of stable and metastable MnS(ZB) form crystallites, no characteristic morphologies were found through TEM.

UV−vis absorption spectra of the metastable MnS nanoparticles, which were ultrasonically dispersed in absolute ethanol, are shown in Figure 4. The width of the absorption band[26] is associated with the dispersion of the particles size (and vibrational coupling).[27] The absorption edge of metastable form nanoparticles (W/ZB) is at 320/340 nm, almost the same as the bulk value of 326 nm (3.80 eV) at 0 K.[28,29] In contrast to the reported value of 375 nm (3.30 eV) at 300 K of thin film,[30] there is a maximum blue shift of 55/35 nm, which can be attributed to the quantum size effect of meta-

(25) Peng, X.; Manna, L.; Yang, W.; Wickham, J.; Scher, E.; Kadavanich, A.; Alivisatos, A. P. *Nature* **2000**, *404*, 59.
(26) Steigerwald, M.; Brus, L. E. *Acc. Chem. Res.* **1990**, *23*, 183.
(27) Trindade, T.; O'Brien, P. *Chem. Mater.* **1997**, *9*, 523.
(28) Wang, L.; Sivannathan, S.; et al. *Phys. Rev. B* **1996**, *54*, 2718.
(29) Goede, O.; Heimbrodt, W.; Lamla, M.; Weinhold, V. *Phys. Status Solidi B* **1988**, *146*, K65.
(30) Ikeda, M.; Wada, H.; Wada, T.; Hirao, T. *Jpn. J. Appl. Phys., Part 1* **1994**, *33*, 4540.

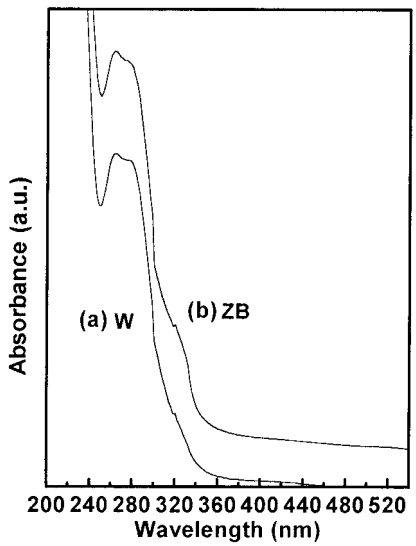


**Figure 4.** UV−vis absorption spectra of metastable MnS nanoparticles.

stable MnS nanocrystallites (the smallest dimension portion of the sample), which were dispersed in the absolute ethanol solution.

Among the first transition metal, the oxides and chalcogenides of manganese are probably the most ionic crystal, because of the manganese $3d^5$ high-spin electronic configuration of spherical symmetry.[31] So, MnS has a fairly great solubility in aqueous solution ($K_{sp} = 3 \times 10^{-10}$ and $3 \times 10^{-13}$ for metastable and stable forms, respectively) in contrast to spare soluble ZnS [$K_{sp} = 2.5 \times 10^{-22}$ ($\beta$) and $1.6 \times 10^{-24}$ ($\alpha$)] and CdS ($K_{sp} = 8.0 \times 10^{-27}$).[32] The metastable form is ready to transform to the stable form above 100 °C, because of the large value of $K_{sp}$ by 3 orders of magnitude in comparison with the stable form. Our experimental results (Table 1) show that, for the solvothermal reaction,

$$MnCl_2 + 4SC(NH_2)_2 \rightarrow MnS \qquad (1)$$

(31) Hulliger, F. *Struct. Bonding* **1968**, *4*, 83.
(32) *Manual of Chemical Analysis* (Chinese); Kexue Press: Beijing, 1997; p 571.

The metastable forms are the primitive phases; in a nonaqueous noncoordinated solvent, such as benzene and THF, the low solubility stabilizes them; in ammonia liquor and ethylenediamine, however, it is undoubtedly that the formation of complex ions $Mn(NH_3)_6^{2+}$ and $Mn(en)_3^{2+}$ is favorable for the transformation to the stable form. It is worth noticing, however, the different metastable forms in benzene and THF. It seems that the MnS(W) phase is ready to be stabilized in a nonpolar hydrocarbon solvent (e.g., benzene) and the MnS(ZB) phase in an ether solvent (e.g., THF). There are still open questions on this subtle difference. Further research is needed, and this will be important to realize the preparation of a single metastable pure phase of MnS, which often coexists in a polycrystalline powder and a thin film.

## 4. Conclusions

Metastable ($\beta$ and $\gamma$) and stable ($\alpha$) MnS crystallites were synthesized by solvothermal reaction in various solvents at 190−200 °C. The rodlike morphologies were found in metastable $\gamma$-MnS(W). Unique "methane-like" four-branched rod clusters were found and characterized. The metastable forms are the primitive phases; in benzene and THF, metastable MnS(W) and MnS(ZB) phases can be prepared; in water, ammonia liquor, and ethylenediamine, however, metastable forms transform to the stable form. Further research is in progress, and this will be important to realize the preparation of a single metastable pure phase of MnS. Because ZnY and CdY (Y = S, Se, and Te) have been successfully synthesized in the solvothermal system,[17−22] it seems that doping of manganese into these group II−VI semiconductors in a solvothermal system at about 200 °C is another mild and simple method to prepare DMS nanocrystallites.

**Acknowledgment.** We are indebted to Prof. Ji Mingrong and Prof. Zheng Huagui for an instructive discussion on the XPS and thermostability analyses. This work is supported by the National Natural Science Foundation of China and the National Nanometer Material Climbing Project.

CM010049J